

## Research Article

# Immunoinformatic Analysis of Calcium-Dependent Protein Kinase 7 (CDPK7) Showed Potential Targets for *Toxoplasma gondii* Vaccine

Ali Taghipour <sup>1</sup>, Sanaz Tavakoli <sup>2</sup>, Mohamad Sabaghan <sup>3</sup>, Masoud Foroutan <sup>4</sup>,  
Hamidreza Majidiani <sup>5</sup>, Shahrzad Soltani <sup>4</sup>, Milad Badri <sup>6</sup>, Ali Dalir Ghaffari <sup>1</sup>,  
and Sheyda Soltani <sup>4</sup>

<sup>1</sup>Department of Parasitology, Faculty of Medical Sciences, Tarbiat Modares University, Tehran, Iran

<sup>2</sup>Department of Parasitology and Mycology, School of Medicine, Isfahan University of Medical Sciences, Isfahan, Iran

<sup>3</sup>Behbahan Faculty of Medical Sciences, Behbahan, Iran

<sup>4</sup>USERN Office, Abadan University of Medical Sciences, Abadan, Iran

<sup>5</sup>Zoonotic Diseases Research Center, Ilam University of Medical Sciences, Ilam, Iran

<sup>6</sup>Medical Microbiology Research Center, Qazvin University of Medical Sciences, Qazvin, Iran

Correspondence should be addressed to Mohamad Sabaghan; [sabaghan.m@ajums.ac.ir](mailto:sabaghan.m@ajums.ac.ir)  
and Masoud Foroutan; [masoud\\_foroutan\\_rad@yahoo.com](mailto:masoud_foroutan_rad@yahoo.com)

Received 10 April 2021; Revised 10 June 2021; Accepted 22 June 2021; Published 12 July 2021

Academic Editor: José F. Silveira

Copyright © 2021 Ali Taghipour et al. This is an open access article distributed under the Creative Commons Attribution License, which permits unrestricted use, distribution, and reproduction in any medium, provided the original work is properly cited.

Apicomplexan parasites, including *Toxoplasma gondii* (*T. gondii*), express different types of calcium-dependent protein kinases (CDPKs), which perform a variety of functions, including attacking and exiting the host cells. In the current bioinformatics study, we have used several web servers to predict the basic features and specifications of the CDPK7 protein. The findings showed that CDPK7 protein has 2133 amino acid residues with an average molecular weight (MW) of 219085.79 D. The aliphatic index with 68.78 and grand average of hydropathicity (GRAVY) with -0.331 score were estimated. The outcomes of current research showed that the CDPK7 protein included 502 alpha-helix, 1311 random coils, and 320 extended strands with GOR4 method. Considering the Ramachandran plot, the favored region contains more than 92% of the amino acid residues. In addition, evaluation of antigenicity and allergenicity showed that CDPK7 protein has immunogenic and nonallergenic nature. The present research provides key data for more animal-model study on the CDPK7 protein to design an efficient vaccine against toxoplasmosis in the future.

## 1. Introduction

*Toxoplasma gondii* is a prevalent intracellular protozoan, which can infect a broad spectrum of mammals (i.e., human) and birds [1, 2]. Oocysts are the potential infective form in the life cycle of the parasite. Feline species as the only definitive hosts can contaminate the environment by shedding unsporulated oocysts through feces [3]. *T. gondii* is transferred by water/vegetables contaminated via mature oocysts and consumption of raw or semicooked meat from infected animals, vertical transmission from infected preg-

nant mothers to neonates, and blood transfusion [4–7]. Approximately one-third of human society has been exposed to *T. gondii*, worldwide [5, 8, 9]. Often *T. gondii* infection among immunocompetent people is asymptomatic or demonstrates mild symptoms, whereas in immunocompromised patients, it can cause a various range of clinical symptoms [6, 9, 10]. Toxoplasmosis in immunocompromised subjects can cause repeated attacks in the brain and manifests as encephalitis [11]. Moreover, toxoplasmosis in pregnant women can cause blindness, microcephaly, and mental retardation in the infant [6, 12]. Different factors, such as host's

MGVQSTRVAGAGGAGGAGPANSIAFSTQLSKECLKYKLFKDFDEFEVL	#	50
KKVYKALSARSPPGDIKETFLOYFPLPLNGERLQKDFKFGSSVDYE	#	100
EFLIGIACVCCRGTSRDMYVLFQVFDLNSDGYIQKSELVAMLNPNLDR	#	150
YMSIRKAQQAHSSEGSNSVGRSGHGKKEEQNLFSQCQRTPNQNGSSGTA	#	200
GAUSSPPNLDDEDEEDTGS CGS NSMFPAQAGGAYPEALVCSDFVP	#	250
SQQYVATGSLSDSTSSNERPRELKPYPHLLARLEQEASSSEGYGR	#	300
SFDEESSGSSYSLSLVFCFSFPHASRNPSPRRVSAQQPTHVGFPEA	#	350
PGQEPGTVSSPTGEGTQAPPAALSSRPSIDSLVSSASSPAGGSPVVLPPP	#	400
VDRPAGAGTGAEFPLQASPHARFAAGDDGSSAGPAGGASGEAARAGAE	#	450
KSPKTGTLQQPRGIIKTAISRTSAIKKETSQSSSTQAPGSPFVRGF	#	500
SQGGSRPVSUPLSRQSSSESVICQGGISVPGSAHANAPPQSGTAPP	#	550
PIVPTSSGGVAPPGVSPPPQVPPVVRAASRAETQENITGEEELGEGA	#	600
TPGDAGREASQKFAAGTGRGSGPLEDEAQNMGLEVPAQAQPSKGPT	#	650
KSAMLLQAEKDKTRQEKAKNPSVAQSLIKEEKEENEKQDVLVDEGIVD	#	700
KIIEECEFHEGKLSFPEFKTLWERNEGLSMFTECLHEEVNGLQGNALY	#	750
RSTSVQSRPRLTAAGLQGFIFKFDPLGSGREGGSGKFRSKLLSSRTSSA	#	800
SFSSRGMKGAGSPSSRVGGFGYSASGGMIVMHHQKVKHLETPAHSS	#	850
RRPRTDLDPATPAPQPSRLSSSPQMATGSSGAASAAGASSVSAGGPA	#	900
ARRSGAQFGAGPNAGALAVSPVSGAELAVGGATPLAGTTFPAHET	#	950
TSQASCHQTPGSGSPGTEASVSVPAAGETISVPSVSVATAVA	#	1000
TQVAGAPTSSAGVEPKQVTVSVSVTVAGGAGSETQPMASVASGSSP	#	1050
AAPGVTGVEAVAVASVPGTFTIGATTAVGVPVSEGPATTPSITLQVITI	#	1100
LDPTTAGAAGAAAAATAAAAAFVEETRAAGGATAPGTSVHTATATAV	#	1150
QGPDPGRGSAGDKVVEAEAFVIGEEGERMGS GDARDDVYERLAGYR	#	1200
HWEQSRMSPQLAVDIVSKELVDFIRSSHQSLHSAELPRDRSPAPSRGALS	#	1250
GASGFGSALASPEGASARAQLPYREGELRQADLAIARAHDDPLACGS	#	1300
HSPRDLYSCPNCNPLLLCPFCBSRYQLTLEGRVMECRQCRLGGSS	#	1350
SSLSDAGAPAGTGANSGAGSADPSGGPAEEDRVEAGICVGGSS	#	1400
RVFTRCWICWELSKAEMKGNSEAIIDGVLKKGKHLHQVQARYVLV	#	1450
DMLYYYRRKGDAPRPFMLEGCVLLEQVGGQGFVAIHPKGETV	#	1500
SKRLLFANSAKEQREWDTLRVATKQALEQLYQVGEQLHGKFSIVYK	#	1550
IHRATNELYAIKVIDKGKINGHERELLREMAILRLLNHPNVIYMKELD	#	1600
TKETLYVMELVRGGLFDLIQQNHLRPELHVNRISQLLSTVYLYHKCG	#	1650
IVHRDLKPENILLDRTNATIKLIDFGLSTLCAPEVHLQPCGTLAYVA	#	1700
PEVLTMEGYNHQVDVWSIGVIMYLLLRGLRFPINQAFGHPSEYENTPVS	#	1750
FDGAVREVSSAKDLIVRMLQPNRRRITVADALQHIWIRNPTAVVNG	#	1800
SRNIDVYISQLDEVHRHSTRGERTMACCEPVFTTIPKNGAKPLQNHGA	#	1850
FVATAGPALARPVQCPAAPAVASAPASSSPSPPTPPESESTPV	#	1900
YAVPAASAPGVSLSGGGLDPAETSVATPVAVSISAPPAARTEGDTGP	#	1950
VEGAAVSSSLPAGSLDEVPESGASLGGESVDAAPVAGREVDLTRGQ	#	2000
QGSTASGVAASPLNLTLQDGSGRMTSATPVVAEAGSPVSGAL	#	2050
LSPAAGSKVSPSPVASPAGVAPSLAAGCSLDLSSASSGTRQRTTEPEA	#	2100
EPARQDERACGTPAEVPAGSPGGSPSIEEVHK	#	2150
#1 . . . . . S . . . . . S . . . . . S . . . . . S . . . . . S . . . . .	#	50
#1 . . . . . S . . . . . S . . . . . T . . . . . S . . . . . S . . . . . Y . . . . .	#	100
#1 . . . . . Y . . . . . S . . . . . S . . . . . Y . . . . . Y . . . . . S . . . . .	#	150
#1 . . . . . SSS . . . . . T . . . . . S . . . . . S . . . . . T . . . . . SS . . . . .	#	200
#1 . . . . . S . . . . . S . . . . . SSS . . . . . Y . . . . .	#	250
#1 . . . . . S . . . . . SS . . . . . S . . . . . S . . . . . T . . . . .	#	300
#1 . . . . . T . . . . . T . . . . . SS . . . . . S . . . . . S . . . . .	#	350
#1 . . . . . T . . . . . S . . . . . S . . . . . S . . . . .	#	400
#1 . . . . . S . . . . . T . . . . . S . . . . . T . . . . . ST . . . . . SST . . . . .	#	450
#1 . . . . . S . . . . . SS . . . . . S . . . . . S . . . . . S . . . . .	#	500
#1 . . . . . S . . . . . S . . . . . S . . . . . T . . . . .	#	550
#1 . . . . . T . . . . . S . . . . . T . . . . . S . . . . .	#	600
#1 . . . . . S . . . . . S . . . . . S . . . . . S . . . . .	#	650
#1 . . . . . S . . . . . T . . . . . S . . . . . S . . . . .	#	700
#1 . . . . . S . . . . . T . . . . . S . . . . . T . . . . .	#	750
#1 . . . . . STS . . . . . S . . . . . S . . . . . S . . . . . SS . . . . . SS . . . . .	#	800
#1 . . . . . S . . . . . SSS . . . . . S . . . . . T . . . . . SS	#	850
#1 . . . . . T . . . . . T . . . . . SSS . . . . . T . . . . . S . . . . .	#	900
#1 . . . . . S . . . . . S . . . . . S . . . . . T . . . . . T	#	950
#1 . . . . . S . . . . . T . . . . . S . . . . . S . . . . .	#	1000
#1 . . . . . T . . . . . S . . . . . T . . . . . T . . . . . S . . . . .	#	1050
#1 . . . . . T . . . . . S . . . . . S . . . . . S . . . . .	#	1100
#1 . . . . . S . . . . . S . . . . . S . . . . . Y . . . . .	#	1150
#1 . . . . . S . . . . . S . . . . . S . . . . . S . . . . . S . . . . .	#	1200
#1 . . . . . S . . . . . S . . . . . S . . . . . S . . . . . S . . . . .	#	1250
#1 . . . . . S . . . . . S . . . . . S . . . . . S . . . . .	#	1300
#1 . . . . . Y . . . . . S . . . . . T . . . . . SS	#	1350
#1 . . . . . SS . . . . . T . . . . . S . . . . . S . . . . .	#	1400
#1 . . . . . T . . . . . S . . . . .	#	1450
#1 . . . . . Y . . . . . T . . . . .	#	1500
#1 . . . . . S . . . . . T . . . . . S . . . . .	#	1550
#1 . . . . . Y . . . . . S . . . . .	#	1600
#1 . . . . . T . . . . . Y . . . . . S . . . . . ST . . . . .	#	1650
#1 . . . . . T . . . . . T . . . . . ST . . . . .	#	1700
#1 . . . . . T . . . . . T . . . . . S . . . . . Y . . . . . T . . . . . S	#	1750
#1 . . . . . SSS . . . . . T . . . . .	#	1800
#1 . . . . . S . . . . . ST . . . . . T . . . . .	#	1850
#1 . . . . . T . . . . . S . . . . . SS . . . . . T . . . . . S . . . . .	#	1900
#1 . . . . . Y . . . . . S . . . . . T . . . . . T . . . . . S . . . . .	#	1950
#1 . . . . . S . . . . . S . . . . . S . . . . . S . . . . .	#	2000
#1 . . . . . ST . . . . . S . . . . . S . . . . . TS . . . . .	#	2050
#1 . . . . . S . . . . . S . . . . . S . . . . . SS . . . . . T . . . . .	#	2100
#1 . . . . . T . . . . . S . . . . . S . . . . .	#	2150

(a)

FIGURE 1: Continued.

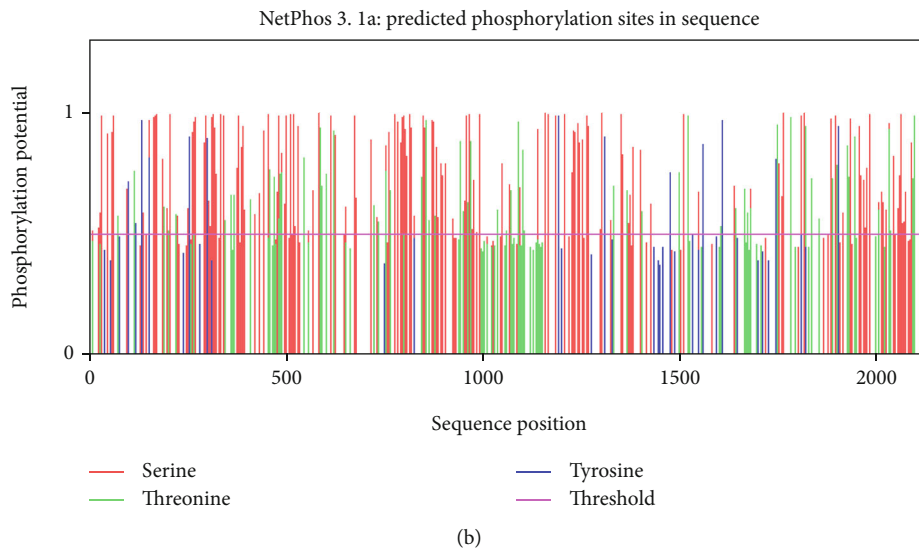


FIGURE 1: NetPhos server output for CDPK7 phosphorylation sites. (a) The number of predicted sites, based on S (serine), T (threonine), and Y (tyrosine); (b) prediction diagram of CDPK7 phosphorylation sites.

TABLE 1: The acylation sites of CDPK7 sequence.

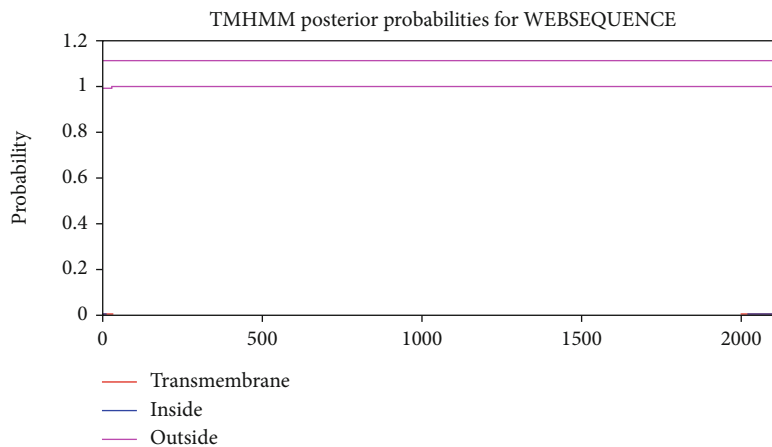
ID	Position	Peptide	Score
TGME49_228750 CDPK7 ( <i>T. gondii</i> )	34	STQLSKECLKQYLKK	1.129
TGME49_228750 CDPK7 ( <i>T. gondii</i> )	109	FLIGIAVCCRGTKSD	1.996
TGME49_228750 CDPK7 ( <i>T. gondii</i> )	110	LIGIAVCCRGTKSDR	5.494
TGME49_228750 CDPK7 ( <i>T. gondii</i> )	187	QNLFSPPQCQRTQPNG	0.526
TGME49_228750 CDPK7 ( <i>T. gondii</i> )	222	DEEDTGSCGSNSNFP	5.293
TGME49_228750 CDPK7 ( <i>T. gondii</i> )	244	YPEAALVCVSDFVPS	3.693
TGME49_228750 CDPK7 ( <i>T. gondii</i> )	321	SLSDVFQCFSDFHA	0.984
TGME49_228750 CDPK7 ( <i>T. gondii</i> )	524	SSEASVICPQGGISP	2.536
TGME49_228750 CDPK7 ( <i>T. gondii</i> )	706	VDKIIEECEFHEHGK	0.403
TGME49_228750 CDPK7 ( <i>T. gondii</i> )	736	ILSMFTECLHEEVWG	1.821
TGME49_228750 CDPK7 ( <i>T. gondii</i> )	1298	AHDDPLACSGHSPRD	5.591
TGME49_228750 CDPK7 ( <i>T. gondii</i> )	1309	SPRDLYSCPNCNPL	1.744
TGME49_228750 CDPK7 ( <i>T. gondii</i> )	1312	DLYSCPNCNPLLLC	8.015
TGME49_228750 CDPK7 ( <i>T. gondii</i> )	1313	LYSCPNCNPLLLCP	7.05
TGME49_228750 CDPK7 ( <i>T. gondii</i> )	1319	CCNPLLLCPFCHSRY	2.719
TGME49_228750 CDPK7 ( <i>T. gondii</i> )	1322	PLLLCPFCHSRYPQL	2.865
TGME49_228750 CDPK7 ( <i>T. gondii</i> )	1340	EGRVVMOCRQCGRLG	2.295
TGME49_228750 CDPK7 ( <i>T. gondii</i> )	1343	VVMOCRQCGRLLGSS	2.929
TGME49_228750 CDPK7 ( <i>T. gondii</i> )	1395	DRVEAGICVGGSSRV	5.406
TGME49_228750 CDPK7 ( <i>T. gondii</i> )	1406	SSRVFTRCWHCWEL	0.108
TGME49_228750 CDPK7 ( <i>T. gondii</i> )	1409	VFTRCWHCWELSKC	1.424
TGME49_228750 CDPK7 ( <i>T. gondii</i> )	1416	CGWELSKCAEMLKGN	4.272
TGME49_228750 CDPK7 ( <i>T. gondii</i> )	1474	GFMFLEGYVELLSE	1.626
TGME49_228750 CDPK7 ( <i>T. gondii</i> )	1649	TVYYLHKCGIVHRDL	1.164
TGME49_228750 CDPK7 ( <i>T. gondii</i> )	1683	DFGLSTLCAPNEVLH	1.6
TGME49_228750 CDPK7 ( <i>T. gondii</i> )	1693	NEVLHQPCGTLAYVA	1.927
TGME49_228750 CDPK7 ( <i>T. gondii</i> )	1828	GEERTMACCPEVPTF	4.139
TGME49_228750 CDPK7 ( <i>T. gondii</i> )	1829	EERTMACCPEVPTFT	7.362
TGME49_228750 CDPK7 ( <i>T. gondii</i> )	2080	PSLAAPGCSDLSSAS	3.862
TGME49_228750 CDPK7 ( <i>T. gondii</i> )	2110	ARQDERACGTAEVP	6.173

```

# WEBSEQUENCE length: 2133
# WEBSEQUENCE number of predicted TMHs: 0
# WEBSEQUENCE exp number of AAs in TMHs: 0.08572999999999999
# WEBSEQUENCE exp number, first 60 AAs: 0.07989
# WEBSEQUENCE total prob of N-in: 0.00375
WEBSEQUENCE TMHMM2.0 outside 1 2133

```

(a)



(b)

FIGURE 2: Transmembrane domains expected in CDPK7 protein. (a) Some statistics and a list of the location of the predicted transmembrane helices and the predicted location of the intervening loop regions. Length: the length of the protein sequence; number of predicted TMHs: the number of predicted transmembrane helices; Exp number of AAs in TMHs: the expected number of amino acids in transmembrane helices. If this number is larger than 18, it is very likely to be a transmembrane protein (or have a signal peptide); Exp number, first 60 AAs: the expected number of amino acids in transmembrane helices in the first 60 amino acids of the protein. If this number is more than a few, you should be warned that a predicted transmembrane helix in the N-term could be a signal peptide; total prob of N-in: the total probability that the N-term is on the cytoplasmic side of the membrane; (b) transmembrane domains expected in CDPK7 protein. (b) Analysis of the transmembrane domains of CDPK7.

immune system status, genetic background, age, gender, contact with infected cats, environmental conditions, and diet and cultural habits, as well as the protozoan genotype, can affect the morbidity and mortality rate of *Toxoplasma* infection [13, 14].

Today, treatment of toxoplasmosis with conventional drugs can just limit the proliferation of tachyzoites at the beginning of infection, while these drugs cannot eradicate cystic forms of parasites in host tissue [15, 16]. In addition, taking these medications in pregnant women can have serious side effects, such as the possibility of teratogenic effects on the fetus [17]. Hence, the discovery and design of an effective vaccine to control and prevent toxoplasmosis is very important, especially in humans and domestic animals. In this regard, various *in silico*-based studies suggest various antigens as suitable candidates for vaccine design [18–32]. Calcium-dependent protein kinases (CDPKs) are a class of serine/threonine kinases that express in apicomplexans, ciliates, and plants [33]. In *T. gondii* as a member of the apicomplexan parasites, several CDPKs have been identified involving in critical functions in the different stages of the life cycle of parasite, including gliding motility (surface translocation), entry into (invasion), and exit from (egress) of host cells [34]. The CDPK7 is a crucial enzyme for division, growth, and maintenance of structural integrity of the *Toxoplasma* centrosome. As a result, TgCDPK7 knockdown is suggested as an important goal in achieving the right vaccine [35].

Computer-aided evaluation of different *T. gondii* proteins involved in various stages of life cycle can open new doors towards recognizing potent vaccine candidates through identification of highly immunogenic, nonallergenic, and nontoxic B- and T-cell epitopes [36]. Thereby, the present *in silico* study was performed to evaluate the crucial biochemical features and immunogenic epitopes of the CDPK7 protein by means of different bioinformatics servers.

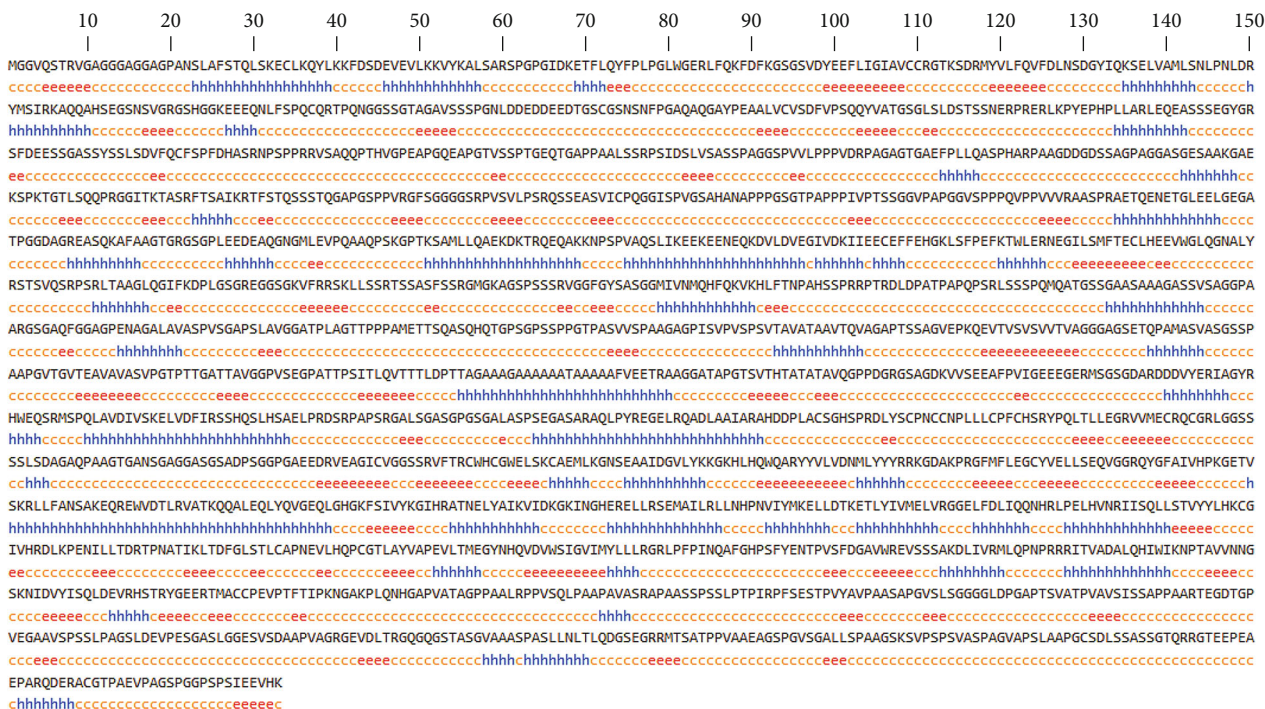
## 2. Methods

**2.1. CDPK7 Sequence.** For this purpose, ToxoDB online website was used to obtain the whole amino acid sequence of *T. gondii* CDPK7 protein.

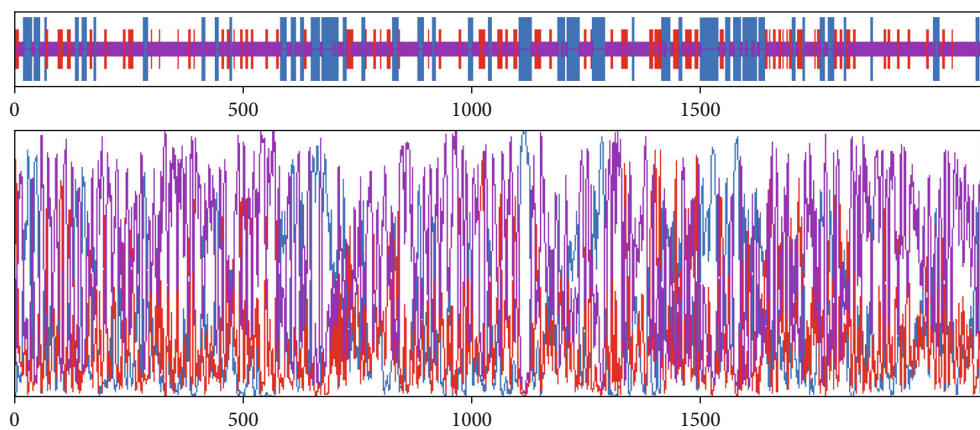
**2.2. Physicochemical Characterization.** We used the ExPASy ProtParam online server to predict the physicochemical parameters of CDPK7 [37].

**2.3. Prediction of Posttranslational Modification (PTM) Sites.** The NetPhos 3.1 online tool was applied to predict phosphorylation location, and the CSS-Palm online server was applied to predict acylation location of the CDPK7 [38, 39].

**2.4. Transmembrane Domains and Subcellular Location.** The transmembrane regions and subcellular localization of *T. gondii* CDPK7 protein were assessed utilizing the TMHMM 2.0 and PSORT II web servers, respectively [38].



(a)



(b)

FIGURE 3: (a) GOR4 server results suggested that CDPK7 encompasses 502 alpha-helix, 320 extended strands, and 1311 random coils in secondary structure; (b) graphical result of the secondary structure prediction of CDPK7 using the GOR4 online server.

2.5. *Secondary and Tertiary Structures.* In this study, we employed the Garnier-Osguthorpe-Robson 4 (GOR4) online tool to forecast the secondary structure of CDPK7 protein [40]. Consequently, the three-dimensional (3D) model structures was used by SWISS-MODEL [38, 41].

2.6. *The 3D Modeled Structure Refinement and Validation.* GalaxyRefine was selected to develop and refine the quality of the template-based protein prediction [42]. To the Ramachandran plot validated the 3D structure of the protein, the SWISS-MODEL software was applied [43]. ProSA-web was used for evaluation of the whole quality of the model [44].

2.7. *Linear and Conformational B-Cell Epitopes.* We used a web-based Bcepred server to predict continuous B-cell epi-

topes exploiting physicochemical characteristics [45]. An online server of ABCpred was applied to predict B-cell epitopes [46]. Using the immune epitope database (IEDB), hydrophilicity [47], Bepipred linear epitope prediction [48], antigenicity [49], surface accessibility [50], beta-turn [51], and flexibility [52] were predicted. Afterwards, discontinuous B-cell epitopes were appraised by ElliPro [53] from the 3D structure of protein epitopes.

2.8. *MHC-I and MHC-II Epitopes.* To this aim, we used the IEDB website to evaluate the half-maximal inhibitory concentration ( $IC_{50}$ ) values of peptides that bind to the main histocompatibility complex (MHC) class I and class II molecules for CDPK7 [54, 55]. All predicted epitopes were then

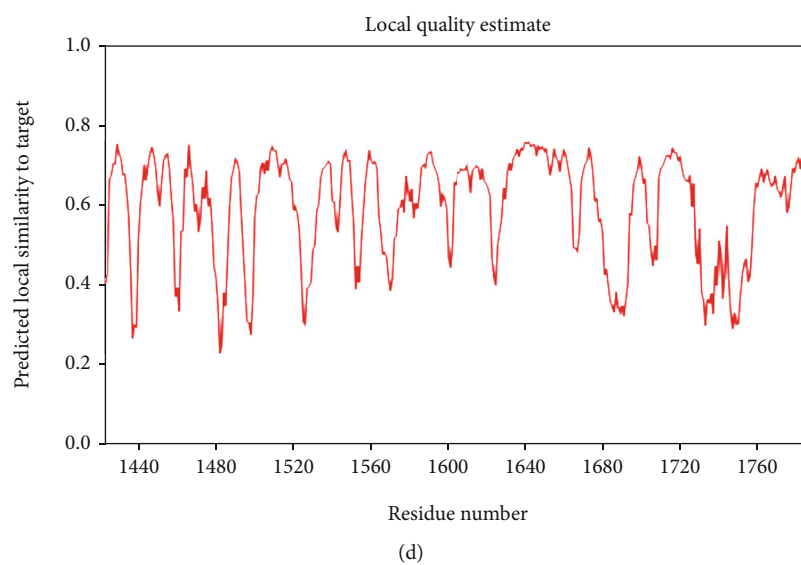
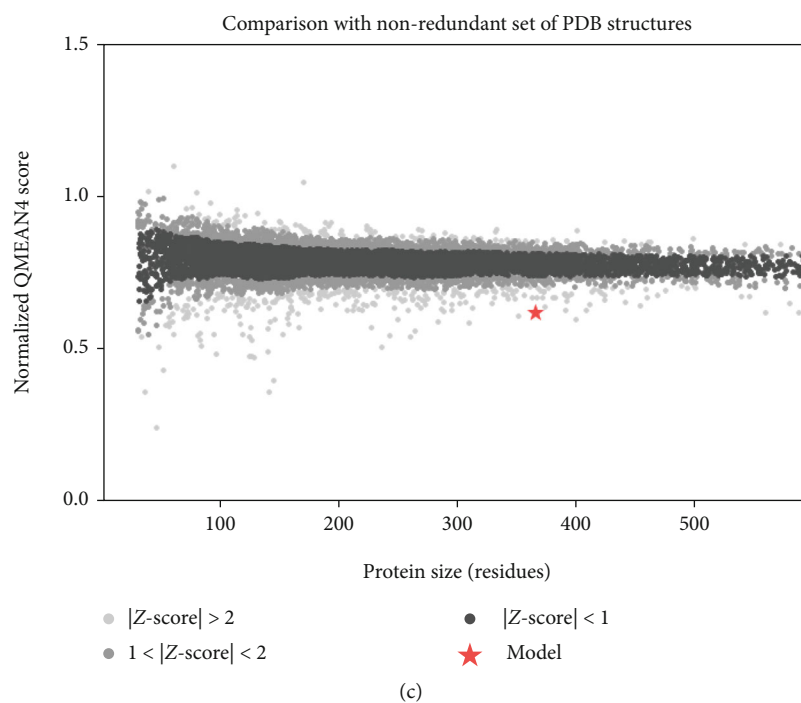
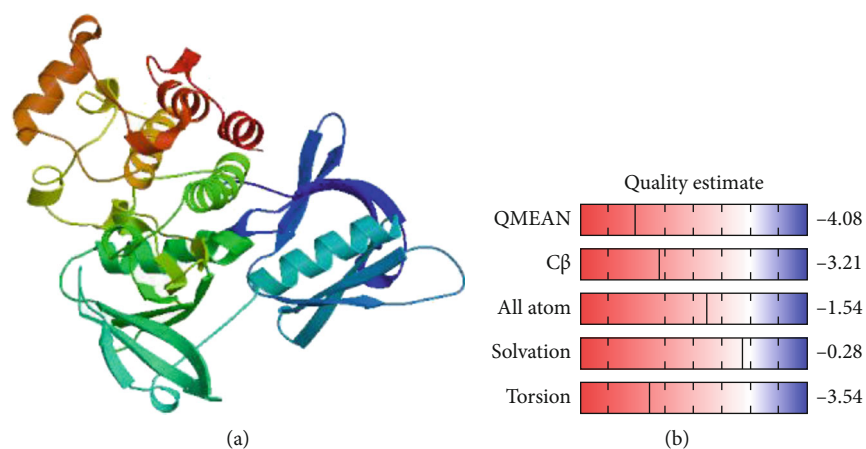


FIGURE 4: SWISS-MODEL server output. (a) Computed 3D model; (b) global quality estimate; (c) comparison with nonredundant set of PDB structures; (d) local quality estimate.

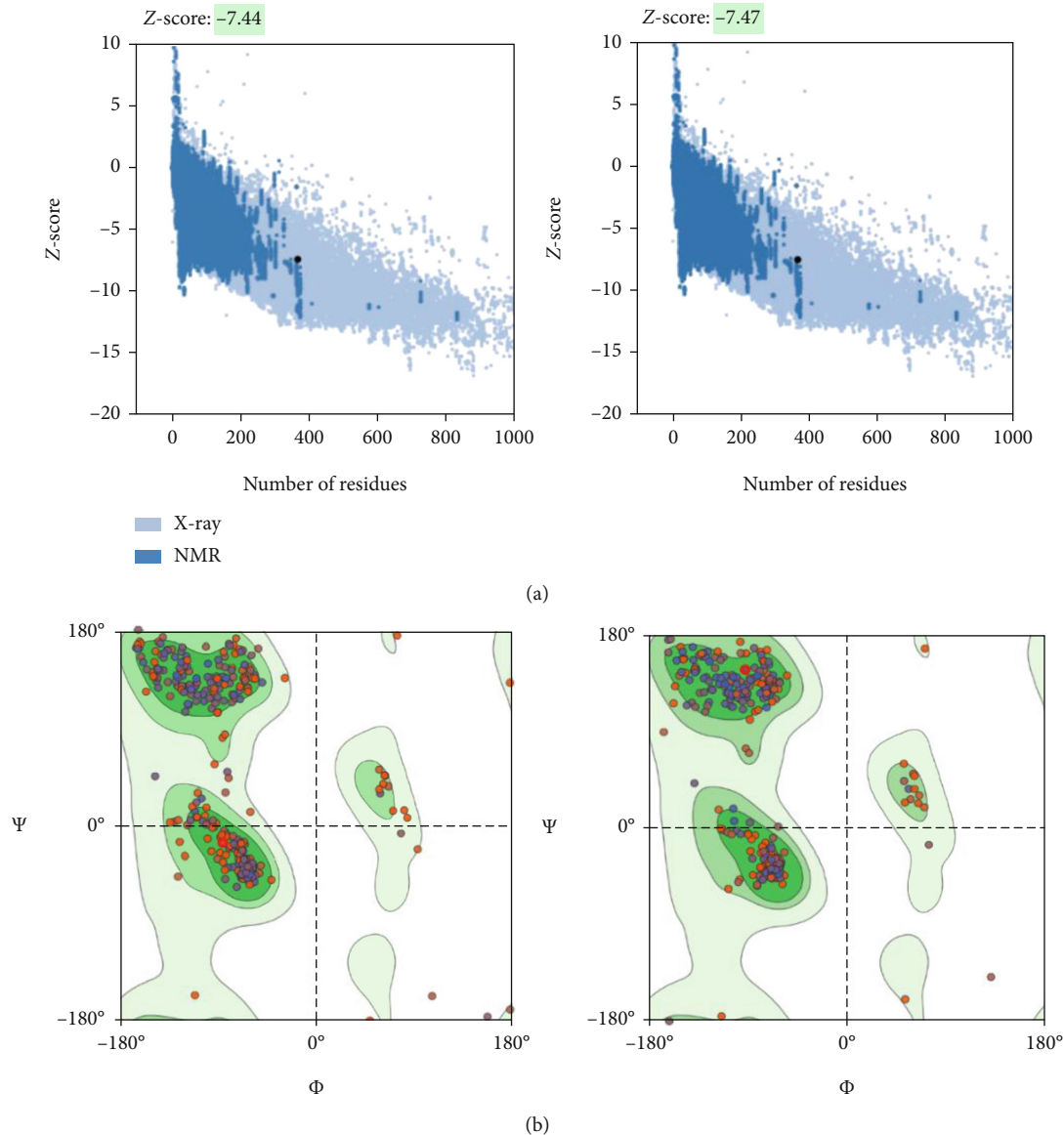


FIGURE 5: Validation of 3D model of CDPK7 protein. (a) The Z-score plot for 3D structure of predicted protein before and after refinement with ProSA-web server, respectively; (b) Ramachandran plot analysis of predicted structure.

evaluated in terms of antigenicity using the VaxiJen v2.0 server.

**2.9. Cytotoxic T-Lymphocyte (CTL) Epitopes.** We applied CTLpred online website according to 75.8% accuracy [56]. Next, all predicted epitopes were evaluated regarding antigenicity using the VaxiJen v2.0 server.

**2.10. Antigenic and Allergenic Profiles.** The antigenicity of the full CDPK7 sequence was estimated by VaxiJen v2.0 [57]. The allergenic profile of CDPK7 was predicted by the AllergenFP v1.0 and AllerTOP v2.0 servers [58, 59].

### 3. Results

**3.1. General Information of CDPK7.** The amino acid structure of CDPK7 was obtained from the ToxoDB server with

accession no. TGME49\_228750. Based on the ProtParam database, the CDPK7 protein entails of 2133 amino acid residues with molecular weight of 219085.79 D, whereas theoretical pI was 5.79. The overall number of negatively (Asp +Glu) charged residues was 209, and positively (Arg+Lys) charged residues was 178. There are a total number of 30441 atoms. The half-life of the CDPK7 was predictable at 30 hours, >20 hours, and >10 hours for mammalian (*in vitro*), yeast (*in vivo*), and *Escherichia coli* (*in vivo*), respectively. In addition, the instability index of the CDPK7 protein presented an unstable nature with a value of 53.28. In addition, the aliphatic index was calculated 68.78, and GRAVY of the protein was estimated -0.331.

**3.2. PTM Sites of CDPK7 Protein.** In the present research, the results exhibited that 269 phosphorylation sites (Thr: 64, Tyr: 13, and Ser: 192) (Figures 1(a) and 1(b)) and 30 acylation

TABLE 2: Epitopes predicted in CDPK7 protein by different parameters based on the Bcipep online server.

Prediction parameter	Epitope sequence
Hydrophilicity	GAGGGAGGAG; KKFDSDEVEV; KGGSDVYEE; CRGTKSDRM; AQAHSEGSNSVGRGSHGGKEEQNL; SPQCQRTPNQNGSSGTAGA; SPGNLDDDEEDTGSCGNSN; SLDTSSNERPRR; EQEASSEGYGRSFDEESSGASSYSS; DHASRNP; GPEAPGQEAAPT; SSTTGEQTGAP; SASSPAGGS; DRPAGAGTAE; RPAAGDDGSSA GAGASGESA AKGAESPKTGT; SOQPRGG; STQSSSTQAGPG; SGGGSRP; PSRQSEASV; SPRAETQENETGLEE; GEGATPGDAGREASQKA; AGTGRGSGPLEDEAQCNG; QPSKGPTKSA; QAEKDKTRQEQAKKNPS; IKEEKEENEQKDV; GSGREGGSGKV; SSRITSSAS; GKAGSPSSRVGG; TNP AHSSPRRTRD; QATGSSGAASA; ARGSGAQ; GGAPENAGA; ETTQASQHQITGSPSSP; GVEPKQE; AGGGAGSETQPA; ASGSPAA; SEGPAIT; DPTTAGA; EETRAAG; QGPPDGRGSA GDVKV; IGEEEGERMSGDARDDDVYER; DSRPAPS; SGASGPGSGA; ASPSEGASAR; ARAHDDP; SGHSPRD; SSSSLDAGAQ; AGTGANSAGGASGADPSGGAEEDRVEAG; KGNSEAA; RRKGDAPKRG; SEQVGGRRQ; KGETVSKR; ANSAKEORE; DKGKING; TDRTPNAT; EVSSAKD; VNNGSKNID; DEVRHSTRYGEERT; AASPSS; DPGAPTS; AARTEGDTGPVEG; DEVPESE; GGESVSDAA; AGRGEVD; TRGQGGSTASG; TLQDGSEGR; AEAGSPG; SSASGTQRRGTEPEAEAPARQDERACGT; GSPGGPS
Flexibility	LAFSTQL; QYLKFKD; KALSARSPG; QKDFDKGSG; AVCRCRTKSD; QQAHSSEGSNSVGRGSHGGKEE; QCQRTPNQNGSSGTAG AVSSPGNLDDDEEDTGSCGNS; SGLSLDTSSNERPR; ARLEQEAASSE; RSFDEESSGA; FDHASRNPSP; GIVSSPTGEO; PAALSSRP; VSASSPAG; PAAAGDDGSS; GPAGGASG; SAAKGAESPKTGTLSQQPRGGITKTA; SAIKRTFTQSSSTQ; PPVRFSGGGGSRP; SVLPSRQSS; NAPPPGSG; PIVPTSSG; PRAETQENE; GDAGREAS; FAAGTGRG; QAAQPSKGT; LQAEKDKTRQEQAKKNP; SLIKEEKEENEQ; ALYRSTSVQSRPS; KDPLGSGREGGSG; SKLSSRTSSAFSSRMGKAGSPSSRV; NPAHSSPRRT; APQPSRLSSPQMATGSS; PAAARGSG; SQHOTGPSGSPSP; TVAGGGAAGSET; ASVASGSS; AVQGGPPDGRGSA; PVIGEEGERMSGGDA; RHWQSR; DFISSH; AELPRDSR; GALSASGPG; LACSGHSP; RQCCRLGGSSSL; TGANSAGG ASGADPSGG; GICVGGSS; AEMILKGN; YYRRKGD; VHPKGETVS; LFANSAKEQ; GKINGHE; ILLTDR; AVVREVSSA; RMLQPNRP; TAVVNNGS; APAAASSP; TPIRPF; PGVSLG; PAARTEGD; SGASLGGESV; VDLTRGQGGSTAG; LTLQDGSEGR; PAAAGSKV; SDSLSSASSGTQRRGTE; VPAGSPGGPS
Accessibility	STQLSKECLKQYLKFKDDEV; VLKVVYKAL; PGIDKETFQY; GERLFQKDFKG; CRGTKSDRMVY; SDGYIQKSEL; NLPNLDRYMSIRKAQQAHSFEG; SHGGKEEQNLSPQCQRTPNQGG; PGNLDDDEEDTG; DSTSSNERPRERLKYEPHPL; ARLEQEAASSEGYGRSFDEESS; DHASRNPSPRRVSAQPPH; PEAPGQE; SPTTGEQTGAPP; PPPVDRPA; QASPHAR; AKGAESPKTGTLSQQPRGGITKTA; ASRTFTQSSSTQ; LPSRQSS; SPPPQVPP; ASPRAETQENETGLEE; GREASQKA; GPLEDEAQQN; PQAAPQSKGPTKSA; LQAEKDKTRQEQAKKNPSV AQLIKEEKEENEQKDVLD; FKTWLERNEG; YRSTSVQSRPSRLTA; REGGSKVFRRSKLLS; GSPSSR; NMQHFQVKH; P AHSSPRRTRDLPATPAPQPSRLSSPMDQ; ETTQASQHQITGPG; GVEP KQEVTV; EETRAAG; QGPPDGRGSA GDKVVSEE; GEEGERMS; SGDARDDDVYERAGYRHWQSRMSPO; RSHQSL; SAELPRDSRPAAPSRG; RAQLPYREGELRQAD; ARAHDDPL; SGHSPRDLYS; CHSRYPQLTL; PEAEDRVEA; VLYKKGKHLHQWQARYY; NMLYYRRKGDAPKRGF; EQVGGRRQ; KGETVSKRL; ANSAKEQREWVD; RVATKQALEQ; IHRATNELY; KVIDKINGHERELRSE; RLLNHPN; KELLDTKETLY; LIQNHRLPEL; VHRDLKPENI; LTDRTPNAT; MEGYNHQ; HPSFENTPVS; RMLQPNRRITV; VNNGSKNID; SQLDEVHSTRYGEERTMA; IPKNGAKPLQNHG; RPFSEST; PPAARTEGDTG; QDGSEGRMSTAT; SKSVPSPS; SSGTQRRGTEPEAEAPARQDERAC; PPSIEE
Turns	SCGNSNFPG; DSTSSNE; YSCPNCNPL; LLNHPNVI
Exposed surface	KECLKQYLKFKDSD; VLKVVYKAL; RGTKSDR; GKEEQNL; DDEDEEDT; SSNERPRERLKYEPHP; RNPSPPRR; AEKSPKTG; LQAEKDKTRQEQAKKNPSV; SLIKEEKEENEQKDV; KVFRRSK; QHFQVKY; SPRRTRDL; EPKQEV; VLYKKGKHLH; LYYRRKGDAPKPR; NSAKEQREW; KQALEQ; KVIDKKG; KELLDTK; HRDLKPEN; LQPNRRIT; QRRGTEE; EPARQDER; EEVHK
Polarity	LSKECLKQYLKFKDSDDEVVLLK; GERLFQKF; RGTKSDR; RYMSIRKAQQAHSFEG; RSHGGKEEQNL; GNLDDDEEDTG; SSNERPRERLKYEPHP; LARLEQEA; GRSDDEES; AEKSPKTG; PRAETQENETGLEE; GREASQKA; GPLEDEAQQ; LQAEKDKTRQEQAKKNP; QSLIKEEKEENEQKDVLDVE; VDKIECEFEFHGKLSF; EFKTWLERNEGIL; FTEKHEEVWGL; REGGSKVFRRSKLLS; QHFQVKHLFT; AHSSPRTRDLD; GVEPKQEV; AFVEETRAAG; DKVVSEE; IGEEEGERMSGDARDDDVYERAGYRHWQSRM; HSAELPRDSR; LPYREGELRQA; IARAHDDPL; EGRVVMFCRQCGR; PGEEDRVEAG; ELSKCAE; LYKKGKHLHQWQ; LYYRRKGDAPKPR; IVHPKGETVSKRL; NSAKEQREWVD; EQLGHGK; VYKGIHRAITNEL; KVIDKINGHERELRSEM; KELLDTK; ELVRGGE; QNHRLPELVNRI; HKCGIVHRDLKPEN; QPNRRITVA; QLDEVHSTRYGEERTMAC; DGSEGRMST; TQRRGTEPEAEAPARQDERAC; PSIEEVHK



TABLE 2: Continued.

Prediction parameter	Epitope sequence
Antigenic propensity	QLSKECLKQYLK; VEVLKKVYK; FLQYFPLPGL; VCCRGTK; MYVLFQVFDL; NLFSPQCQ; LVCVSDVFVPSQYV; YEPHPLL; YSSLSDFVQCFSFDFH; PSIDSLVS; GGSPPVLPVPPVD; SRPVSVLPSRQS; SVIC;POGG; PPIVPTS; VSPPQVPPVVVR; QKDVL DVEGIV; ECLHEEVW; FQKVKHLF; GPISVPVSPSVT; QEVTVSVSVTV; PSITLQVTTTL; IVSKELVDFIRS; PRDLYSCPNCCNPLLLCPFCHSRYPQLTLEGRVVMECRQCGR; ICVGGSS; VFTRCWHC; IDGVLYK; RYYVLVDNML; FLEGCYVELLSEQV; TVSKRLLF; LEQLYQV; GKFSIVYKGIH; IRLLNHPNV; KETLYIVMELVR; LFDLIQQ;
	RLPELHVNRJISQLLSTVYYLHKCGIVHRD; FGLSTLC; EVLHQPCGTL; YNHQVDVWSIGVIMYLLLRGRL; LIVRMLQ; IDVVYISQLD; CCPVPTPE; LRPPVSQLP; VSPSSLP; SLLNLTLQ; SVPSPSV

TABLE 3: The predicted B-cell epitopes via the ABCpred tool.

Rank	Sequence	Start position	Score
1	SSPPGTPASVVSPAAGAGPI	965	0.95
1	EVPQAAQPSKGPTKSAMLLQ	638	0.95
1	GGVSPPPQPPVVVRAASPR	564	0.95
1	GETVSKRLLFANSACEQREW	1497	0.95
2	DVLDVEGIVDKIIIECEFFE	691	0.94
2	EEDEAQNGMLEVPQAAQPS	627	0.94
2	GAPTSVATPVAVSISSAPPA	1922	0.94
3	KNGAKPLQNHGAPVATAGPP	1839	0.93
4	ALEQLYQVGEQLGHGKFSIV	1528	0.92
5	GAPSLAVGGATPLAGTTPPP	927	0.91
5	FGYSASGGMIVNMQHFKVK	821	0.91
5	KDKTRQEQAKKNPSPAQSL	660	0.91
5	EDTGSCGNSNFPQAQAQGA	217	0.91
5	LPAAPAVASRAPAASSPSSL	1868	0.91
5	DVWSIGVIMYLLLRGRLPPF	1714	0.91
5	VYKGIHRATNELYAIKVIDK	1547	0.91
5	SAKEQREWVDTLRVATKQQA	1509	0.91
6	TPVYAVPAASAPGVSLSGGG	1898	0.90
6	LIQNHRLPELHVNRISQL	1620	0.90
6	SGDARDDDVYERIAGYRHWE	1184	0.90
6	VAGAPTSSAGVEPKQEVTVS	1003	0.90
7	QATGSSGAASAAAGASSVSA	877	0.89
7	RSKLLSSRTSSASFSSRGMG	789	0.89
7	VGSAHANAPPPSGTAPPPP	532	0.89
7	LYYYRRKGDAPRGFMFLEG	1454	0.89
8	AGALAVASPVSGAPSLAVGG	916	0.88
8	PAAGDDGDSSAGPAGGASGE	424	0.88
8	SEAAIDGVLYKKGKHLHQWQ	1424	0.88
9	KNPSPAQSLIKEEKEENEQ	670	0.87
9	GGDAGREASQKFAAAGTGRRG	603	0.87
9	SAGPAGGASGESAAKGAEKS	433	0.87
9	ASRNPSPPRRVSAQQPTHVG	328	0.87
9	PHPLLARLEQEASSSEGYGR	281	0.87
9	SSNERPRERLKPYPHPLLA	267	0.87
9	TPAEVPAGSPGGSPSIEEV	2112	0.87
9	SSLSDAQAAPAGTGANSGA	1351	0.87
9	KQEVTVSVSVTVAGGGAGS	1016	0.87
10	STSVQSRPSRLTAAGLQGIF	752	0.86
10	LIKEEKEENEQKDVLDVEGI	679	0.86
10	LQASPHARPAAGDDGDSSAG	416	0.86
10	AQAQGAYPEAALVCVDFVP	231	0.86
10	GEERTMACCEVPTFTIPKN	1821	0.86
10	RCWHCGWELSKCAEMLKGNS	1405	0.86
10	MSPQLAVDIVSKELVDFIRS	1207	0.86
10	VASGSSPAAPGVTGVTEAVA	1044	0.86
11	TQGAPGSPVVRGFSGGGSR	488	0.85
11	KTASRFTSAIKRTFSTQSSS	468	0.85
11	EESGASSYSSLDVDFQCFS	304	0.85

TABLE 3: Continued.

Rank	Sequence	Start position	Score
11	GSPGVSGALLSPAAGSKSVP	2042	0.85
11	GDKVVSEEAFVIGEEGER	1161	0.85
12	ISVPVSPSVTAVATAAVTQV	984	0.84
12	NMQHFQKVKHLFTNPAHSSP	832	0.84
12	ASQKAFAGAAGTGRGSGPLEED	610	0.84
12	VEETRAAGGATAPGTSVTHHT	1125	0.84
12	TVAGGGAGSETQPAMASVAS	1027	0.84
13	DKIIECEFFEHGKLSFPEF	700	0.83
13	PGIDKETFLQYFPLPLWGE	64	0.83
13	GYRHWEQSRMSPQLAVDIVS	1198	0.83
13	TTGATTAVGGPVSEGPATTP	1072	0.83
14	QTGPSGPSSPPGTPASVVSP	958	0.82
14	GTLSQQPRGGITKTASRFTS	456	0.82
14	AGAVSSSPGNLDDDEDEEDT	200	0.82
14	PCGTLAYVAPEVLTMEGYNH	1692	0.82
14	NSVGRGSHGGKEEQNLFSF	166	0.82
14	LLSTVYYLHKCGIVHRDLKP	1639	0.82
14	GFAIVHPKGETVSKRLLFAN	1489	0.82
14	GFMFLEGCYVELLSEQVGGGR	1467	0.82
14	CRQCGRLGGSSSLSDAQAQ	1340	0.82
14	LSGASGPGSGALASPSSEGAS	1249	0.82
14	KELVDFIRSSHQSLHSAELP	1218	0.82
14	ATAAAAAAFVEETRAAGGATA	1117	0.82
14	AGAAAAAATAAAAAFVEETR	1110	0.82
15	DPATPAPQPSRLSSSPQMQA	859	0.81
15	FFEHGKLSFPEFKTWLERNE	708	0.81
15	TGLEELGEGATPGGDAGREA	591	0.81
15	APPAALSSRPSIDSLVSASS	369	0.81
15	SPTGEQTGAPPAALSSRPSI	361	0.81
15	EEPEAEPARQDERACGTPAE	2096	0.81
15	PAARTEGDTGPVEGA AVSPS	1940	0.81
15	KAQQAHSSEGSNSVGRGSHGG	156	0.81
15	VGGPVSEGPATTPSITLQVT	1079	0.81
16	SGSVDYEEFLIGI VCCRGT	94	0.80
16	ICPQGGISPVGSAHANAPPP	523	0.80
16	VQSTRVGAGGGAGGAGPANS	4	0.80
16	ASSSEGYGRSFDEESSGASS	292	0.80
16	GESVSDAAPVAGRGEVDLTR	1978	0.80
17	PAPPPIVPTSSGGVPAPGGV	547	0.79
17	GGGSRPVSVLPSRQSEASV	503	0.79
17	SATPPVAAEAGSPGVSGALL	2032	0.79
17	NHGAPVATAGPPAALRPPVS	1847	0.79
17	LFSPQCQRTPNQGGSSGTAG	182	0.79
17	LLLRGRLPPINQAFGHPSF	1724	0.79
17	ELVRGGELFDLIQQNHRLPE	1610	0.79
17	NELYAIKVIDKGKINGHERE	1556	0.79
17	AAIARAHDDPLACSGHSPRD	1286	0.79
17	EAVAVASVPGTPTTGATTAV	1060	0.79

TABLE 3: Continued.

Rank	Sequence	Start position	Score
18	PSKGPTKSAMLLQAEKDKTR	645	0.78
18	QEAPGTVSSPTGEQTGAPPA	353	0.78
18	APGCSDLSSASSGTQRRGTE	2077	0.78
18	ASPASLLNLTLDGSEGRRM	2011	0.78
18	DEVRHSTRYGEERTMACCPE	1812	0.78
18	VHRDLKPENILLTDRTPNAT	1652	0.78
18	GGASGSADPSGGPGAEDRV	1371	0.78
19	PSRQSSEASVICPQGGSIPV	513	0.77
19	AAVSPSSLPAGSLDEVPESE	1954	0.77
19	YENTPVSFDAVWREVSSSA	1744	0.77
19	ETLYIVMELVRGELFDLIQ	1603	0.77
19	LLSEQVGGRRQYGAIVHPKG	1478	0.77
19	GASARAQLPYREGELRQADL	1266	0.77
20	PLPGLWGERLFQKFDKGGSG	76	0.76
20	PRAETQENETGLEELGEGAT	582	0.76
20	FGLSTLCAPNEVLHQPCGTL	1677	0.76
20	ATIKLTDGFLSTLCAPNEVL	1670	0.76
20	KHLHQWQARYYVLVDNMLYY	1437	0.76
20	CSGHSPRDLYSCPNCNPLL	1298	0.76
20	AGGGAGGAGPANSALFSTQL	11	0.76
21	GREGGSGKVFRRSKLLSSRT	778	0.75
21	VCVSDFVPSQQYVATGSGLS	243	0.75
21	AVSISAPPAARTEGDTGPV	1932	0.75
21	KNIDVYISQLDEVHSTRYG	1802	0.75
21	ELVAMLSNLPNLDRYMSIRK	137	0.75
21	REGELRQADLAAIARAHDDP	1276	0.75
21	VFDLNSDGYIQKSELVAMLS	124	0.75
21	TAPGTSVTHATATAVQGGPP	1135	0.75

sites (Table 1) were recognized in the CDPK7, representing that the CDPK7 sequence is composed of 299 possible PTM sites.

**3.3. Transmembrane Domains and Subcellular Location.** Based on the TMHMM output, no transmembrane domain was found for CDPK7 (Figures 2(a) and 2(b)). Moreover, by PSORT II, the CDPK7 subcellular site was predicted as follows: 78.3% nuclear, 8.7% cytoplasmic, 8.7% plasma membrane, and 4.3% cytoskeletal.

**3.4. Secondary and Tertiary Structures.** The secondary structure of CDPK7 was predicted via the GOR4 online server, suggesting 502 alpha-helix, 320 extended strands, and 1311 random coils (Figures 3(a) and 3(b)). Moreover, the SWISS-MODEL analysis is shown in Figures 4(a)–4(d).

**3.5. Refinement and Validation of Tertiary Structure.** Protein validation by means of the SWISS-MODEL server displayed that 92.86% of residues were situated in favored regions and 1.65% in the outlier regions. According to the Ramachandran plot, there were 97.80% residues in the favored

region with 0.27% residues in the outlier regions of the refined model (Figure 5).

**3.6. Predicted Linear and Discontinuous B-Cell Epitopes of the CDPK7 Protein.** The predicted linear B-cell epitopes by the Bcepred are listed in Table 2. The outputs of the ABCpred server are tabulated in Table 3 (only the epitopes over scores of 0.75 are embedded in Table 3). The higher peptide score proposes the greater chance of being an epitope. The present server estimated 124 epitopes over 0.75 scores on the sequence, in which the linear epitope SSPPGTPASVV-SPAAGAGPI (score: 0.95) had the greatest score. Four epitopes with over 0.95 scores were as follows: “SSPPGTPASVVSPAAGAGPI,” “EVPQAAQPSKGPTK-SAMLLQ,” “GGVSPPPQVPPVVVRAASPR,” and “GETVSKRLLFANSMAKEQREW.” The average score of antigenicity, beta-turn, flexibility, hydrophilicity, Bepipred linear epitope prediction, and surface accessibility for the CDPK7 protein using the IEDB online server was 1.026, 1.042, 1.017, 2.396, 0.350, and 1.00, respectively (Figure 6). Five discontinuous B-cell epitopes were predicted using the ElliPro server (Table 4).

**3.7. MHC-Binding Epitopes.** The results are listed in Tables 5 and 6. Epitopes were assessed regarding antigenicity, and those highly antigenic epitopes were finally selected.

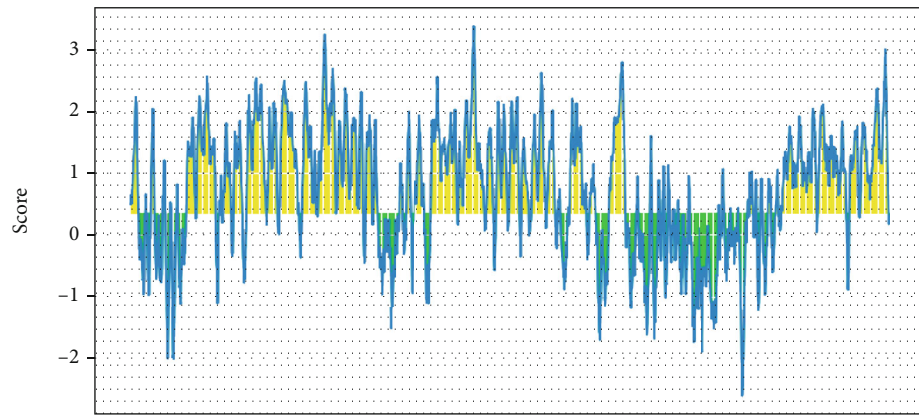
**3.8. CTL Epitope Prediction.** The high-ranked CTL epitopes predicted by the CTLpred tool for CDPK7 protein are summarized in Table 7. Epitopes were assessed regarding antigenicity, and those highly antigenic epitopes were finally selected.

**3.9. Antigenic and Allergenic Profiles.** The antigenic profile of CDPK7 was conducted by the VaxiJen web server with score of 0.7074 (threshold: 0.5). Based on AllergenFP and AllerTOP v2.0 analyses, the CDPK7 protein was appraised as possible nonallergen.

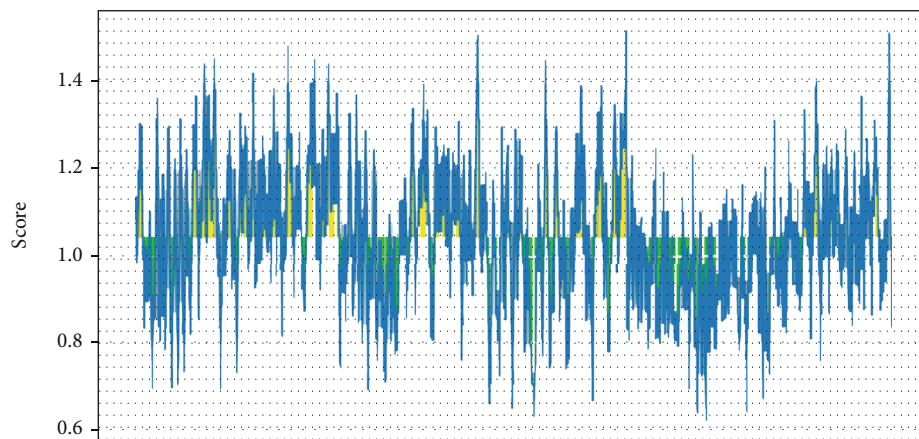
## 4. Discussion

Toxoplasmosis is a significant menace to human society as well as livestock industry [2, 8, 60]. Thus, the design and improvement of an efficient vaccine against *T. gondii* infection is still a great challenge for researchers against toxoplasmosis in domestic animals and humans [61]. Recently, bioinformatics tools are more focused for rational vaccine design, with some advantage, including the following: (i) time- and cost-effectiveness; (ii) accurately targeting, long-lasting immunity with favorable polarity in cellular components; and (iii) elimination of undesired responses through specific, epitope-based construct design. Nevertheless, the obtained *in silico* results are only theoretical data which must be confirmed using wet lab experiments inevitably [62].

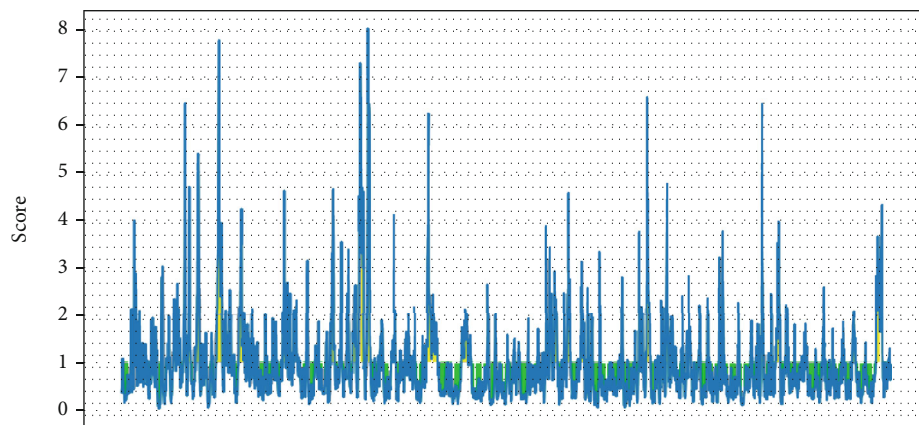
It has been known that CDPK7 contributes to several functions in *T. gondii* such as gliding movement, host-cell invasion, and egress as well as other vital growth processes [34]. Here, we conducted a comprehensive analysis of TgCDPK7, a member of the CDPK family in *T. gondii*. The



Position  
(a)



Position  
(b)



Position  
(c)

FIGURE 6: Continued.

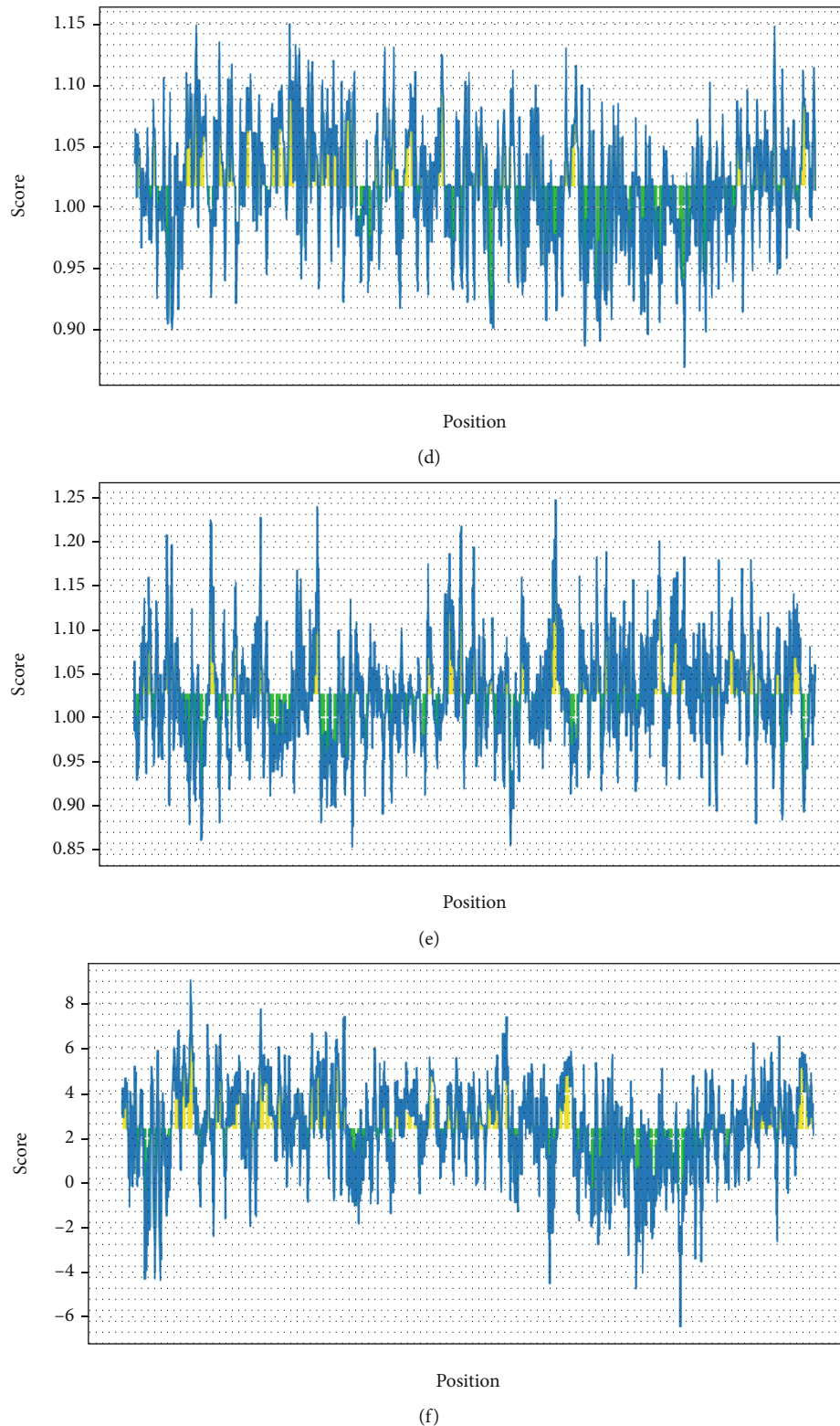


FIGURE 6: Propensity scale plots of CDPK7 protein. (a) Bepipred linear; (b) beta-turn; (c) surface accessibility; (d) flexibility; (e) antigenicity; (f) hydrophilicity.  $x$ -axis and  $y$ -axis represent position and score, respectively. The horizontal line indicates the threshold or the average score. Yellow colors (above the threshold) indicate favorable regions related to the properties of interest. Green color (below the threshold) indicates the unfavorable regions related to the properties of interest.

TABLE 4: Conformational B-cell epitopes of CDPK7 protein predicted by the ElliPro server.

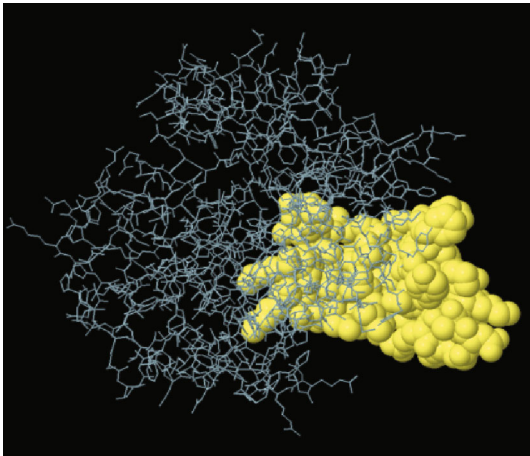
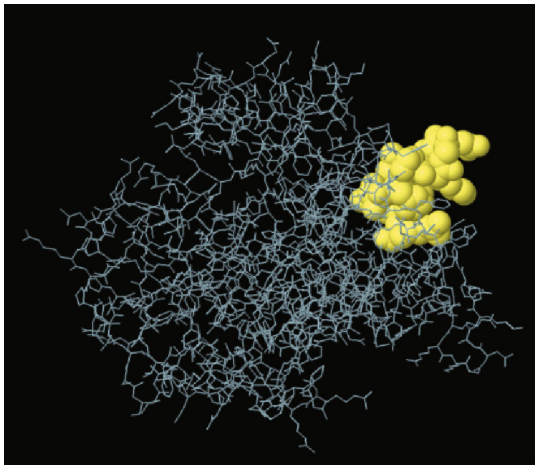
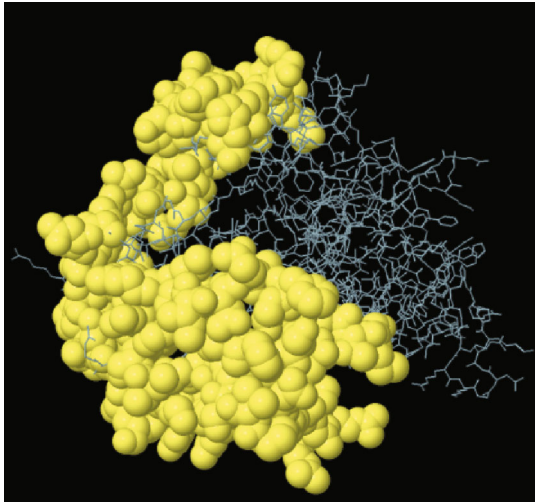
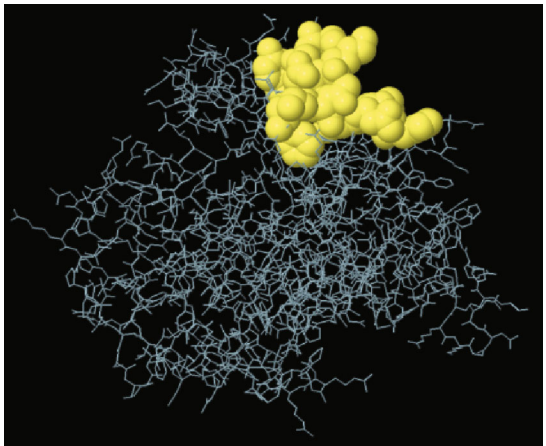
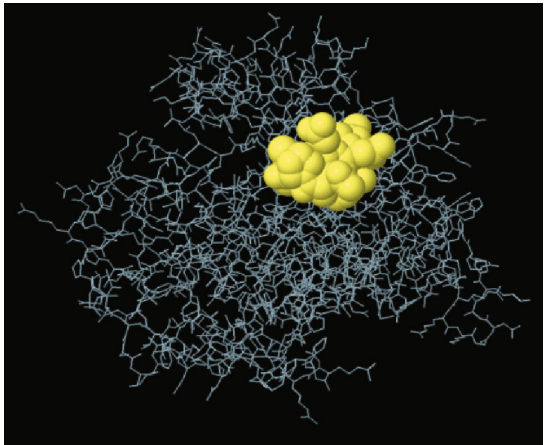
Residues	Number of residues	Score	3D structure
A:V1431, A:L1432, A:Y1433, A:K1434, A:K1435, A:G1436, A:K1437, A:H1438, A:L1439, A:H1440, A:Q1441, A:W1442, A:Q1443, A:A1444, A:R1445, A:Y1456, A:Y1457, A:R1458, A:R1459, A:K1460, A:G1461, A:D1462, A:A1463, A:K1464, A:P1465, A:R1466, A:G1467, A:F1468, A:E1477, A:L1478, A:L1479, A:S1480, A:E1481, A:Q1482, A:V1483, A:G1484, A:G1485, A:R1486, A:Q1487, A:Y1488, A:G1489, A:L1504, A:L1505, A:F1506, A:A1507, A:N1508, A:S1509, A:A1510, A:K1511, A:Q1513, A:R1514	51	0.82	
A:V1493, A:H1494, A:P1495, A:K1496, A:G1497, A:E1498, A:T1499, A:V1500, A:S1501, A:K1502, A:R1503	11	0.755	
A:A1528, A:L1529, A:E1530, A:Q1531, A:L1532, A:Y1533, A:Q1534, A:V1535, A:G1536, A:E1537, A:Q1538, A:H1541, A:I1546, A:Y1548, A:K1549, A:G1550, A:I1551, A:H1552, A:R1553, A:A1554, A:T1555, A:N1556, A:E1557, A:L1558, A:L1611, A:V1612, A:R1613, A:G1614, A:Q1623, A:N1624, A:H1625, A:L1627, A:P1628, A:E1629, A:L1630, A:H1631, A:N1633, A:R1634, A:T1664, A:D1665, A:R1666, A:T1667, A:P1668, A:N1669, A:A1670, A:V1699, A:A1700, A:P1701, A:L1704, A:T1705, A:M1706, A:L1726, A:R1727, A:G1728, A:R1729, A:L1730, A:P1731, A:F1732, A:P1733, A:I1734, A:N1735, A:Q1736, A:A1737, A:F1738, A:G1739, A:P1741, A:S1742, A:F1743, A:Y1744, A:E1745, A:N1746, A:T1747, A:P1748, A:V1749, A:S1750, A:F1751, A:D1752, A:G1753, A:A1754, A:V1755, A:W1756, A:E1758, A:V1759, A:S1760, A:S1761, A:S1762, A:A1763, A:K1764, A:D1765, A:V1768, A:R1769, A:L1771, A:Q1772, A:P1773, A:N1774, A:P1775, A:R1776, A:R1777, A:R1778	99	0.677	

TABLE 4: Continued.

Residues	Number of residues	Score	3D structure
A:F1544, A:D1565, A:K1566, A:G1567, A:K1568, A:I1569, A:N1570, A:G1571, A:H1572, A:E1603, A:T1604, A:Y1606	12	0.645	
A:C1683, A:A1684, A:P1685, A:N1686, A:E1687, A:V1688, A:L1689, A:Q1691, A:P1692, A:C1693	10	0.535	

amino acid sequence of CDPK7 comprises 2133 residues with an average MW of 219085.79 D, which characterizes a suitable antigenic nature (the peptides with MW more than 10 kDa are considered as good immunogens) [63]. According to the ExPasy ProtParam server, GRAVY and the aliphatic index of the CDPK7 were achieved at -0.331 and 68.78, respectively. In summary, the great value of aliphatic index means that the peptide has more stability in a broad range of various temperatures. Moreover, the low/negative value of the GRAVY factor signifies the better interaction of peptide with the molecules of water. It is efficient to identify that PTMs have a fundamental role in cell stability [64]. The acquired outcomes show that CDPK7 comprises 299 potential PTM sites (269 phosphorylation and 30 acylation positions), representing that these positions may organize protein activity.

To predict the secondary structure of CDPK7, the GOR4 tool was recruited. The results of secondary structure of CDPK7 verified and included 502 (out of 2133) alpha-helix, 320 extended strands, and 1311 random coils. It is known that the key role of the proteins is related to their three-dimensional structure. As such, to comprehend the influ-

ences between both structures and functions, assessment of 3D structure is the key aim of expecting a protein's nature [65].

Humoral and cellular immunity are strongly stimulated in *T. gondii* infection [66, 67], in such a way that the establishment of IgG antibodies avoids the protozoan from attachment to the receptors of host cell [67]. Interferon- $\gamma$  (IFN- $\gamma$ ), CD $_4^+$ , and CD $_8^+$  T cells as the main members of T cells play a dynamic role in constraining acute and chronic infection. These major cytokines prevent the reactivation of bradyzoites in the host tissue cyst [66]. Epitope prediction has critical value to evaluate the specificity of antigen. Furthermore, epitope evaluation may reveal the pathogenesis and immune process of the pathogen in design vaccine researches [65, 68]. The strength of using *in silico* is the detection of the component epitopes that are critical for the interaction of antibodies and antigens. Several linear B-cell epitopes were predicted by the ABCpred server, among which those epitopes above 0.9 score were of great significance to be included in multi-epitope vaccine constructs. Moreover, we applied the IEDB online server to evaluate the IC $_50$  values of peptides that link to the MHC class I/II molecules for CDPK7. According to the

TABLE 5: IC<sub>50</sub> values for CDPK7 binding to MHC class I molecules obtained using the IEDB<sup>a</sup>.

MHC-II allele <sup>b</sup>	Start-stop <sup>c</sup> CDPK7	Peptide sequence	Percentile rank <sup>d</sup> CDPK7	Antigenicity
H2-Db	1882-1891	SSPSSLPTPI	0.15	0.4079
	143-152	SNLPNLDRYM	0.21	-0.4284
	1637-1646	SQLLSTVYYL*	0.24	0.9146
H2-Dd	647-656	KGPTKSAMLL*	0.18	0.9201
	1612-1621	VRGGELFDLI	0.28	0.1770
	1483-1492	VGGRQYGFAI	0.64	0.1561
H2-Kb	1721-1730	IMYLLLRGRL*	0.55	1.4751
	798-807	SSASFSSRGM*	1.0	1.3623
	1643-1652	VYYLHKCGIV	1.2	0.1373
H2-Kd	1474-1483	CYVELLSEQV*	0.79	0.5079
	1445-1454	RYYVLVDNML*	1.15	0.9079
	822-831	GYSASGGMIV*	1.3	0.9579
H2-Kk	1555-1564	TNELYAIKVI	0.12	0.2695
	1084-1093	SEGPATPSI	0.75	0.2366
	694-703	DVEGIVDKII	1.5	0.1511
H2-Ld	1589-1598	HPNVIYMKEL	3.8	0.2773
	1729-1738	RLPFPINQAF	4.2	0.3317
	279-288	YEPHLLARL	4.6	0.1027

<sup>a</sup>The immune epitope database (<http://tools.iedb.org/mhci/>). <sup>b</sup>H2-Db, H2-Dd, H2-Kb, H2-Kd, H2-Kk, and H2-Ld alleles are mouse MHC class I molecules. <sup>c</sup>Ten amino acids for analysis were used each time. <sup>d</sup>Low percentile rank = high level binding; high percentile rank = low level binding; IC<sub>50</sub> values = percentile rank. \* indicates potential antigenic epitopes (threshold = 0.5).

TABLE 6: IC<sub>50</sub> values for CDPK7 binding to MHC class II molecules obtained using the IEDB<sup>a</sup>.

MHC-II allele <sup>b</sup>	Start-stop <sup>c</sup> CDPK7	Peptide sequence	Percentile rank <sup>d</sup> CDPK7	Antigenicity
H2-IAb	1109-1123	AAGAAAAAATAAAAA*	0.07	0.8045
	1108-1122	AAAGAAAAAATAAAAA*	0.08	0.8354
	1110-1124	AGAAAAAATAAAAAF*	0.08	0.7176
H2-IAd	1035-1049	SETQPAMASVASGSS*	0.13	0.6766
	1034-1048	GSETQPAMASVASGS*	0.15	0.7059
	1036-1050	ETQPAMASVASGSSP*	0.25	0.6536
H2-IEd	1451-1465	DNMLYYRRKGDACP*	0.14	0.6972
	1452-1466	NMLYYRRKGDACP*	0.14	0.8298
	1450-1464	VDNMLYYRRKGDACP*	0.19	0.6159

<sup>a</sup>The immune epitope database (<http://tools.immuneepitope.org/mhcii/>). <sup>b</sup>H2-IAb, H2-IAd, and H2-IEd alleles are mouse MHC class II molecules. <sup>c</sup>Fifteen amino acids for analysis were used each time. <sup>d</sup>Low percentile rank = high level binding; high percentile rank = low level binding; IC<sub>50</sub> values = percentile rank. \* indicates potential antigenic epitopes (threshold = 0.5).

obtained results from IEDB, the T-cell epitopes on CDPK7 have the capability to bind intensely to MHC class I and class II molecules. It is important to note that the lower IC<sub>50</sub> values show the higher-level of affinity, which show an appropriate T-cell epitope.

Other the main stage, CTLpred is a special approach used to predict CTL epitopes, which is important in vaccine-

related studies. This tool relies on elegant machine learning methods, such as ANN and SVM. We recognized the CTL epitopes using the CTLpred online database to select the top CDPK7 epitopes. The CTLpred server utilizes consensus and combined estimates, in line with these two methods [56]. Evaluation of antigenicity and allergenicity showed that CDPK7 protein has immunogenic and nonallergenic nature.



TABLE 7: Predicted CDPK7 epitopes by CTLpred<sup>a</sup>.

Peptide rank	Start position <sup>b</sup>	Sequence	Score (ANN/SVM) <sup>c</sup>	Antigenicity
1	280	EPHLLARL	0.83/1.3591088	0.0131
2	1716	WSIGVIMYL	0.96/1.1120848	0.1711
3	1398	GSSRVFTRC	0.94/1.0685326	-0.7197
4	1187	ARDDDVYER	0.65/1.3441588	0.3493
5	715	SFPEFKTWL*	0.98/0.95345497	1.0485
6	1763	AKDLIVRML*	0.98/0.89030833	0.8096
7	724	ERNEGILSM*	0.65/1.0757075	0.5393
8	470	ASRFTSAIK*	0.80/0.85963689	1.0303
9	1573	ERELRSEM*	0.51/1.0720792	0.9337
10	1188	RDDDVYERI	0.85/0.73017891	0.0942
11	1666	RTPNATIKL	0.99/0.58481613	0.2323
12	32	KECLKQYLK*	0.99/0.58376856	1.2628
13	1411	WELSKCAEM	0.19/1.3750392	0.3168
14	1749	VSFDGAVWR*	0.96/0.59370426	1.2284
15	743	GLQGNALYR*	0.99/0.54484483	1.4369

<sup>a</sup>CTLpred, available online at <http://www.imtech.res.in/raghava/ctlpred/index.html>. <sup>b</sup>Nine amino acids for analysis were used. <sup>c</sup>The default artificial neural network (ANN) and support vector machine (SVM) cut-off scores were set 0.51 and 0.36, respectively. \* indicates potential antigenic epitopes (threshold = 0.5).

## 5. Conclusion

Well antigenicity, hydrophilicity, surface accessibility, and flexibility indexes were detected for CDPK7. Hence, we recommend that a suitable vaccine should be designed and verified both *in silico* and *in vivo* by the potential B- and T-cell epitopes predicted in this study.

## Abbreviations

3D:	Three-dimensional
ACC:	Auto cross covariance
ANN:	Artificial neural network
CD:	Cluster of differentiation
CDPK:	Calcium-dependent protein kinase
CTL:	Cytotoxic T-lymphocyte
GOR:	Garnier-Osguthorpe-Robson
GRAVY:	Grand average of hydropathicity
IC <sub>50</sub> :	Half-maximal inhibitory concentration
IEDB:	Immune epitope database
IFN- $\gamma$ :	Interferon- $\gamma$
MHC:	Major histocompatibility complex
MW:	Molecular weight
PDB:	Protein data bank
pI:	Isoelectric point
PTM:	Post-translational modification
SVM:	Support vector machine
<i>T. gondii</i> :	<i>Toxoplasma gondii</i> .

## Data Availability

The datasets used and/or analysed during the current study are available from the corresponding author on reasonable request.

## Ethical Approval

This study received the approval from the Behbahan Faculty of Medical Sciences Ethical Committee (IR.BHN.REC.1399.034).

## Disclosure

The funders of this study had no role in the study design, analysis and interpretation of data, writing of the final paper, and the decision to submit the manuscript for publication. The corresponding author had access to the data in the study and had final responsibility for the decision to submit for publication.

## Conflicts of Interest

The authors declare that there is no conflict of interest.

## Acknowledgments

This study was financially supported by the Behbahan Faculty of Medical Sciences, Behbahan, Iran (Grant No. 99013).

## References

- [1] J. P. Dubey, "The history of *Toxoplasma gondii* The first 100 years," *The Journal of Eukaryotic Microbiology*, vol. 55, no. 6, pp. 467–475, 2008.
- [2] M. Foroutan, Y. Fakhri, S. M. Riahi et al., "The global seroprevalence of *Toxoplasma gondii* in pigs: A systematic review and meta-analysis," *Veterinary Parasitology*, vol. 269, pp. 42–52, 2019.
- [3] J. Dubey, "History of the discovery of the life cycle of *Toxoplasma gondii*," *International Journal for Parasitology*, vol. 39, no. 8, pp. 877–882, 2009.

- [4] K. Shapiro, L. Bahia-Oliveira, B. Dixon et al., "Environmental transmission of *Toxoplasma gondii*: Oocysts in water, soil and food," *Food and Waterborne Parasitology*, vol. 15, article e00049, 2019.
- [5] M. Foroutan-Rad, H. Majidiani, S. Dalvand et al., "Toxoplasmosis in blood donors: a systematic review and meta-analysis," *Transfusion Medicine Reviews*, vol. 30, no. 3, pp. 116–122, 2016.
- [6] A. Rostami, S. M. Riahi, D. G. Contopoulos-Ioannidis et al., "Acute *Toxoplasma* infection in pregnant women worldwide: a systematic review and meta-analysis," *PLoS Neglected Tropical Diseases*, vol. 13, no. 10, article e0007807, 2019.
- [7] B. Maleki, N. Ahmadi, M. Olfatifar et al., "Toxoplasma oocysts in the soil of public places worldwide: a systematic review and meta-analysis," *Transactions of the Royal Society of Tropical Medicine and Hygiene*, vol. 115, no. 5, pp. 471–481, 2021.
- [8] A. Rostami, S. M. Riahi, H. R. Gamble et al., "Global prevalence of latent toxoplasmosis in pregnant women: a systematic review and meta-analysis," *Clinical Microbiology and Infection*, vol. 26, no. 6, pp. 673–683, 2020.
- [9] Z. D. Wang, H. H. Liu, Z. X. Ma et al., "Toxoplasma gondii infection in immunocompromised patients: a systematic review and meta-analysis," *Frontiers in Microbiology*, vol. 8, p. 389, 2017.
- [10] S. Soltani, M. S. Kahvaz, S. Soltani, F. Maghsoudi, and M. Foroutan, "Seroprevalence and associated risk factors of *Toxoplasma gondii* infection in patients undergoing hemodialysis and healthy group," *BMC Research Notes*, vol. 13, no. 1, p. 551, 2020.
- [11] H. Furrer, M. Opravil, E. Bernasconi, A. Telenti, and M. Egger, "Stopping primary prophylaxis in HIV-1-infected patients at high risk of toxoplasma encephalitis," *The Lancet*, vol. 355, no. 9222, pp. 2217–2218, 2000.
- [12] S. Fallahi, A. Rostami, M. Nourollahpour Shiadeh, H. Behniafar, and S. Paktinat, "An updated literature review on maternal-fetal and reproductive disorders of *Toxoplasma gondii* infection," *Journal of Gynecology Obstetrics and Human Reproduction*, vol. 47, no. 3, pp. 133–140, 2018.
- [13] R. Silva, H. Langoni, and J. Megid, "Adaptive and genetic evolution of *Toxoplasma gondii*: a host-parasite interaction," *Revista da Sociedade Brasileira de Medicina Tropical*, vol. 50, no. 4, pp. 580–581, 2017.
- [14] L. Galal, D. Ajzenberg, A. Hamidović, M. F. Durieux, M. L. Dardé, and A. Mercier, "*Toxoplasma* and Africa: One Parasite, Two Opposite Population Structures," *Trends in Parasitology*, vol. 34, no. 2, pp. 140–154, 2018.
- [15] M. Antczak, K. Dzitko, and H. Długońska, "Human toxoplasmosis—Searching for novel chemotherapeutics," *Bio-medicine & Pharmacotherapy*, vol. 82, pp. 677–684, 2016.
- [16] S. Rajapakse, M. Chrishan Shivanthan, N. Samaranayake, C. Rodrigo, and S. Deepika Fernando, "Antibiotics for human toxoplasmosis: a systematic review of randomized trials," *Pathogens and Global Health*, vol. 107, no. 4, pp. 162–169, 2013.
- [17] P. Valentini, M. Annunziata, D. F. Angelone et al., "Role of spiramycin/cotrimoxazole association in the mother-to-child transmission of toxoplasmosis infection in pregnancy," *European Journal of Clinical Microbiology & Infectious Diseases*, vol. 28, no. 3, pp. 297–300, 2009.
- [18] N.-Z. Zhang, M. Wang, Y. Xu, E. Petersen, and X. Q. Zhu, "Recent advances in developing vaccines against *Toxoplasma gondii*: an update," *Expert Review of Vaccines*, vol. 14, no. 12, pp. 1609–1621, 2015.
- [19] M. Foroutan, L. Zaki, S. Tavakoli, S. Soltani, A. Taghipour, and F. Ghaffarifar, "Rhomboid antigens are promising targets in the vaccine development against *Toxoplasma gondii*," *EXCLI Journal*, vol. 18, pp. 259–272, 2019.
- [20] M. Foroutan, F. Ghaffarifar, Z. Sharifi, A. Dalimi, and O. Jorjani, "Rhoptry antigens as *Toxoplasma gondii* vaccine target," *Clinical and Experimental Vaccine Research*, vol. 8, no. 1, pp. 4–26, 2019.
- [21] M. Foroutan, L. Zaki, and F. Ghaffarifar, "Recent progress in microneme-based vaccines development against *Toxoplasma gondii*," *Clinical and Experimental Vaccine Research*, vol. 7, no. 2, pp. 93–103, 2018.
- [22] A. Asghari, S. Shamsinia, H. Nourmohammadi et al., "Development of a chimeric vaccine candidate based on *Toxoplasma gondii* major surface antigen 1 and apicoplast proteins using comprehensive immunoinformatics approaches," *European Journal of Pharmaceutical Sciences*, vol. 162, p. 105837, 2021.
- [23] M. C. Nosrati, E. Ghasemi, M. Shams et al., "*Toxoplasma gondii* ROP38 protein: Bioinformatics analysis for vaccine design improvement against toxoplasmosis," *Microbial Pathogenesis*, vol. 149, p. 104488, 2020.
- [24] H. Can, S. Erkunt Alak, A. E. Köseoğlu, M. Döşkaya, and C. Ün, "Do *Toxoplasma gondii* apicoplast proteins have antigenic potential? An *in silico* study," *Computational Biology and Chemistry*, vol. 84, p. 107158, 2020.
- [25] A. D. Ghaffari, A. Dalimi, F. Ghaffarifar, M. Pirestani, and H. Majidiani, "Immunoinformatic analysis of immunogenic B- and T-cell epitopes of MIC4 protein to designing a vaccine candidate against *Toxoplasma gondii* through an *in-silico* approach," *Clinical and Experimental Vaccine Research*, vol. 10, no. 1, pp. 59–77, 2021.
- [26] H. Majidiani, A. Dalimi, F. Ghaffarifar, M. Pirestani, and A. D. Ghaffari, "Computational probing of *Toxoplasma gondii* major surface antigen 1 (SAG1) for enhanced vaccine design against toxoplasmosis," *Microbial Pathogenesis*, vol. 147, p. 104386, 2020.
- [27] A. D. Ghaffari, A. Dalimi, F. Ghaffarifar, and M. Pirestani, "Structural prediction and antigenic analysis of ROP16 protein utilizing immunoinformatics methods in order to identification of a vaccine against *Toxoplasma gondii*: An *in silico* approach," *Microbial Pathogenesis*, vol. 142, p. 104079, 2020.
- [28] A. D. Ghaffari, A. Dalimi, F. Ghaffarifar, and M. Pirestani, "Antigenic properties of dense granule antigen 12 protein using bioinformatics tools in order to improve vaccine design against *Toxoplasma gondii*," *Clinical and Experimental Vaccine Research*, vol. 9, no. 2, pp. 81–96, 2020.
- [29] M. Foroutan, A. D. Ghaffari, S. Soltani, H. Majidiani, A. Taghipour, and M. Sabaghan, "Bioinformatics analysis of calcium-dependent protein kinase 4 (CDPK4) as *Toxoplasma gondii* vaccine target," *BMC Research Notes*, vol. 14, no. 1, p. 50, 2021.
- [30] M. Khodadadi, F. Ghaffarifar, A. Dalimi, and E. Ahmadpour, "Immunogenicity of *in-silico* designed multi-epitope DNA vaccine encoding SAG1, SAG3 and SAG5 of *Toxoplasma gondii* adjuvanted with CpG-ODN against acute toxoplasmosis in BALB/c mice," *Acta Tropica*, vol. 216, p. 105836, 2021.
- [31] M. Foroutan, F. Ghaffarifar, Z. Sharifi, and A. Dalimi, "Vaccination with a novel multi-epitope ROP8 DNA vaccine against acute *Toxoplasma gondii* infection induces strong B and T cell

- responses in mice," *Comparative Immunology, Microbiology and Infectious Diseases*, vol. 69, p. 101413, 2020.
- [32] M. Foroutan, F. Ghaffarifar, Z. Sharifi, A. Dalimi, and M. Pirestani, "Bioinformatics analysis of ROP8 protein to improve vaccine design against *Toxoplasma gondii*," *Infection, Genetics and Evolution*, vol. 62, pp. 193–204, 2018.
- [33] M. Tzen, R. Benarous, J. Dupouy-Camet, and M. P. Roisin, "A novel *Toxoplasma gondii* calcium-dependent protein kinase," *Parasite*, vol. 14, no. 2, pp. 141–147, 2007.
- [34] M. Foroutan and F. Ghaffarifar, "Calcium-dependent protein kinases are potential targets for *Toxoplasma gondii* vaccine," *Clinical and experimental vaccine research*, vol. 7, no. 1, pp. 24–36, 2018.
- [35] J. Morlon-Guyot, L. Berry, C. T. Chen, M. J. Gubbels, M. Lebrun, and W. Daher, "The *Toxoplasma gondii* calcium-dependent protein kinase 7 is involved in early steps of parasite division and is crucial for parasite survival," *Cellular Microbiology*, vol. 16, no. 1, pp. 95–114, 2014.
- [36] D. R. Flower, "Computer-aided vaccine design," *Human Vaccines & Immunotherapeutics*, vol. 10, no. 1, pp. 241–243, 2014.
- [37] E. Gasteiger, C. Hoogland, A. Gattiker et al., "Protein Identification and Analysis Tools on the ExPASy Server," in *The proteomics protocols handbook*, pp. 571–607, Springer, 2005.
- [38] J. Zhou, L. Wang, A. Zhou et al., "Bioinformatics analysis and expression of a novel protein ROP48 in *Toxoplasma gondii*," *Acta Parasitologica*, vol. 61, no. 2, pp. 319–328, 2016.
- [39] H. Majidiani, S. Soltani, A. D. Ghaffari, M. Sabaghan, A. Taghipour, and M. Foroutan, "In-depth computational analysis of calcium-dependent protein kinase 3 of *Toxoplasma gondii* provides promising targets for vaccination," *Clin Exp Vaccine Res*, vol. 9, no. 2, pp. 146–158, 2020.
- [40] J. Garnier, J.-F. Gibrat, and B. Robson, "GOR method for predicting protein secondary structure from amino acid sequence," in *Methods Enzymol*, pp. 540–553, Elsevier, 1996.
- [41] N. Guex, M. C. Peitsch, and T. Schwede, "Automated comparative protein structure modeling with SWISS-MODEL and Swiss-PdbViewer: a historical perspective," *Electrophoresis*, vol. 30, no. S1, pp. S162–S173, 2009.
- [42] H. Park and C. Seok, "Refinement of unreliable local regions in template-based protein models," *Proteins: Structure, Function, and Bioinformatics*, vol. 80, pp. 1974–1986, 2012.
- [43] M. Bertoni, F. Kiefer, M. Biasini, L. Bordoli, and T. Schwede, "Modeling protein quaternary structure of homo- and hetero-oligomers beyond binary interactions by homology," *Scientific Reports*, vol. 7, no. 1, p. 10480, 2017.
- [44] M. Wiederstein and M. J. Sippl, "ProSA-web: interactive web service for the recognition of errors in three-dimensional structures of proteins," *Nucleic Acids Research*, vol. 35, no. Web Server, pp. W407–W410, 2007.
- [45] S. Saha and G. P. S. Raghava, "BcePred: prediction of continuous B-cell epitopes in antigenic sequences using physico-chemical properties," in *International Conference on Artificial Immune Systems*, pp. 197–204, Springer, 2004.
- [46] S. Saha and G. P. S. Raghava, "Prediction of continuous B-cell epitopes in an antigen using recurrent neural network," *Proteins: Structure, Function, and Bioinformatics*, vol. 65, no. 1, pp. 40–48, 2006.
- [47] J. M. R. Parker, D. Guo, and R. S. Hodges, "New hydrophilicity scale derived from high-performance liquid chromatography peptide retention data: correlation of predicted surface residues with antigenicity and X-ray-derived accessible sites," *Biochemistry*, vol. 25, no. 19, pp. 5425–5432, 1986.
- [48] J. E. P. Larsen, O. Lund, and M. Nielsen, "Improved method for predicting linear B-cell epitopes," *Immuno Research*, vol. 2, no. 1, p. 2, 2006.
- [49] A. Kolaskar and P. C. Tongaonkar, "A semi-empirical method for prediction of antigenic determinants on protein antigens," *FEBS Letters*, vol. 276, no. 1-2, pp. 172–174, 1990.
- [50] E. A. Emini, J. V. Hughes, D. Perlow, and J. Boger, "Induction of hepatitis A virus-neutralizing antibody by a virus-specific synthetic peptide," *Journal of Virology*, vol. 55, no. 3, pp. 836–839, 1985.
- [51] P. Y. Chou and G. D. Fasman, "Prediction of the secondary structure of proteins from their amino acid sequence," *Advances in Enzymology and Related Areas of Molecular Biology*, vol. 47, pp. 45–148, 1978.
- [52] P. Karplus and G. E. Schulz, "Prediction of chain flexibility in proteins," *Naturwissenschaften*, vol. 72, no. 4, pp. 212–213, 1985.
- [53] J. Ponomarenko, H.-H. Bui, W. Li et al., "ElliPro: a new structure-based tool for the prediction of antibody epitopes," *BMC Bioinformatics*, vol. 9, no. 1, p. 514, 2008.
- [54] M. Andreatta and M. Nielsen, "Gapped sequence alignment using artificial neural networks: application to the MHC class I system," *Bioinformatics*, vol. 32, no. 4, pp. 511–517, 2016.
- [55] P. Wang, J. Sidney, C. Dow, B. Mothé, A. Sette, and B. Peters, "A systematic assessment of MHC class II peptide binding predictions and evaluation of a consensus approach," *PLoS Computational Biology*, vol. 4, no. 4, article e1000048, 2008.
- [56] M. Bhasin and G. P. S. Raghava, "Prediction of CTL epitopes using QM, SVM and ANN techniques," *Vaccine*, vol. 22, no. 23-24, pp. 3195–3204, 2004.
- [57] I. A. Doytchinova and D. R. Flower, "VaxiJen: a server for prediction of protective antigens, tumour antigens and subunit vaccines," *BMC Bioinformatics*, vol. 8, no. 1, p. 4, 2007.
- [58] I. Dimitrov, L. Naneva, I. Doytchinova, and I. Bangov, "AllergenFP: allergenicity prediction by descriptor fingerprints," *Bioinformatics*, vol. 30, no. 6, pp. 846–851, 2014.
- [59] I. Dimitrov, D. R. Flower, and I. Doytchinova, "AllerTOP-a server for in silico prediction of allergens," in *BMC bioinformatics*, p. S4, BioMed Central, 2013.
- [60] S. Stelzer, W. Basso, J. Benavides Silván et al., "*Toxoplasma gondii* infection and toxoplasmosis in farm animals: Risk factors and economic impact," *Food and Waterborne Parasitology*, vol. 15, article e00037, 2019.
- [61] F. Rezaei, S. Sarvi, M. Sharif et al., "A systematic review of *Toxoplasma gondii* antigens to find the best vaccine candidates for immunization," *Microbial Pathogenesis*, vol. 126, pp. 172–184, 2019.
- [62] S. Parvizpour, M. M. Pourseif, J. Razmara, M. A. Rafi, and Y. Omid, "Epitope-based vaccine design: a comprehensive overview of bioinformatics approaches," *Drug Discovery Today*, vol. 25, no. 6, pp. 1034–1042, 2020.
- [63] J. Berzofsky and I. Berkower, "Antigen-antibody interaction," in *Fundamental immunology*, pp. 595–644, Raven Press, New York, 1984.
- [64] T.-Y. Lee, J. B.-K. Hsu, W.-C. Chang, T. Y. Wang, P. C. Hsu, and H. D. Huang, "A comprehensive resource for integrating and displaying protein post-translational modifications," *BMC Research Notes*, vol. 2, no. 1, p. 111, 2009.

- [65] Y. Wang, G. Wang, J. Cai, and H. Yin, "Review on the identification and role of *Toxoplasma gondii* antigenic epitopes," *Parasitology Research*, vol. 115, no. 2, pp. 459–468, 2016.
- [66] I. El-Kady, "T-cell immunity in human chronic toxoplasmosis," *Journal of the Egyptian Society of Parasitology*, vol. 41, no. 1, pp. 17–28, 2011.
- [67] P. C. Sayles, G. W. Gibson, and L. L. Johnson, "B cells are essential for vaccination-induced resistance to virulent *Toxoplasma gondii*," *Infection and Immunity*, vol. 68, no. 3, pp. 1026–1033, 2000.
- [68] D. Xu and Y. Zhang, "Improving the physical realism and structural accuracy of protein models by a two-step atomic-level energy minimization," *Biophysical Journal*, vol. 101, no. 10, pp. 2525–2534, 2011.